Naturwissenschaften (2009) 96:1385–1391
DOI 10.1007/s00114-009-0585-y

ORIGINAL PAPER

Seeing it coming: infants' brain responses to looming danger

F. R. (Ruud) van der Weel · Audrey L. H. van der Meer

Received: 24 April 2009 / Revised: 18 June 2009 / Accepted: 19 June 2009 / Published online: 15 September 2009

Abstract A fundamental property of most animals is the ability to see whether an object is approaching on a direct collision course and, if so, when it will collide. Using high-density electroencephalography in 5- to 11-month-old infants and a looming stimulus approaching under three different accelerations, we investigated how the young human nervous system extracts and processes information for impending collision. Here, we show that infants' looming related brain activity is characterised by theta oscillations. Source analyses reveal clear localised activity in the visual cortex. Analysing the temporal dynamics of the source waveform, we provide evidence that the temporal structure of different looming stimuli is sustained during processing in the more mature infant brain, providing infants with increasingly veridical time-to-collision information about looming danger as they grow older and become more mobile.

Keywords Looming · Infants · High-density EEG · Theta oscillations · Source analysis · Tau-coupling analysis · Timing in the brain

Introduction

How does the infant brain sense looming danger? Throughout the animal kingdom, the sight of a rapidly approaching object usually signals danger and elicits avoidance reactions (Schiff et al. 1962; Schiff 1965; Martinoya and Delius 1990). An approaching object on a direct collision course projects an expanding image on the retina, providing information that the object is approaching on a collision course and how imminent the collision is. Animal data about the types of neurons that react to such looming stimuli come from studies on the locust (Hatsopoulos et al. 1995; Rind and Simmons 1997) and the pigeon (Sun and Frost 1998). Looming stimuli creating travelling waves of neural activity in the visual cortex have been measured in adults (Dougherty et al. 2003), and there is ample evidence that the human visual system is specialised to detect and respond to approaching as opposed to receding motion (Morrone et al. 2000; Ptito et al. 2001; Shirai and Yamaguchi 2004; Holliday and Meese 2005). Using functional magnetic resonance imaging, neural activation in response to collision judgments has been reported in left inferior parietal cortex (Assmus et al. 2003; Coull et al. 2008), left ventral pre-motor cortex (Coull et al. 2008) and left sensorimotor cortex (Field and Wann 2005), suggesting these areas to be critically involved in temporal prediction.

Infants are also in need of neural structures allowing them to judge impending collisions adequately, especially as their mobility increases during the second half of the first year of life. Behavioural studies on blinking to visual stimuli on collision course (Kayed and Van der Meer 2007) and discrimination of changes in heading from optic flow (Gilmore et al. 2004) show that prior to the onset of locomotion, infants have problems timing the blink and are less sensitive to optical collisions and flow. Recent developments in non-evasive, high-density electroencephalography (EEG) with sufficiently high temporal resolution allow us to investigate how timing information for impending collision is processed in the infant brain. Research on animal spatial

Electronic supplementary material The online version of this article (doi:10.1007/s00114-009-0585-y) contains supplementary material, which is available to authorized users.

F. R. van der Weel (✉) · A. L. H. van der Meer
Developmental Neuroscience Laboratory,
Department of Psychology,
Norwegian University of Science and Technology,
N-7491 Trondheim, Norway
e-mail: ruudw@svt.ntnu.no

navigation (O'Keefe and Recce 1993; Mehta et al. 2002) highlights the role of theta oscillations in providing a temporal code, suggesting that there is spatial information in the precise timing of spikes with respect to the theta rhythm. In infancy, theta activity is strongly related to cognitive and anticipatory attentional processes (Orekhova et al. 1999). Based on these findings, we explore the possibility that event-related theta activity in the infant brain can provide the infant with information for impending collision.

Materials and methods

We recorded EEG activity using a Geodesic Sensor Net 200 (Tucker 1993) comprising 126 electrodes evenly distributed across the scalp. The vertex electrode (Cz) served as a reference and the EEG was sampled at 500 Hz. During the entire experiment, corneal reflection (Tobii ×50) was used to record gaze of both eyes (50 Hz), and trials in which infants did not look for the entire stimulus duration were excluded from further analyses. A total of 22 healthy, full-term pre-locomotor 5–7-, 8–9- and crawling 10–11-month-old infants were recruited from newspaper birth announcements. Eighteen (12 boys) provided data for the final sample, six in each age group. Parents gave their informed written consent prior to inclusion in the study according to the Helsinki Declaration. The experimental setup is shown in Fig. 1 and Supplementary Video 1.

A total of 502 trials where the looming stimulus approached the infants on a direct collision course under three different constant accelerations were recorded. Animals have an evolved bias for looming events. Similar to findings obtained from the nucleus rotundus of pigeons (Sun and Frost 1998) and the auditory cortex in monkeys (Maier and Ghazanfar 2007), additional control trials where the virtual object's trajectory did not approach on a direct collision course but contracted (Holliday and Meese 2005) or veered to the left or right elicited on a trial-by-trial basis either no (in the case of contraction) or much smaller evoked responses that were compromised by head and eye movements (in the case of veering) in our infant participants and were therefore not included in the present analyses. Infants were very impressed with our looming stimulus and frequently blinked to protect their eyes. EEG records were inspected for artefacts or poor recordings, and trials were eliminated from the analyses if they occurred. Out of 440 remaining trials, each infant contributed on average 24 (standard deviation (SD)=6) trials to the analysis, more or less evenly distributed amongst the three looms and the three age groups.

Results and discussion

In order to specifically locate brain activity in response to looming, we applied brain electrical source analysis (BESA 5.1, MEGIS software GmbH; Hoechstetter et al. 2004). The BESA algorithm estimates the location and the orientation

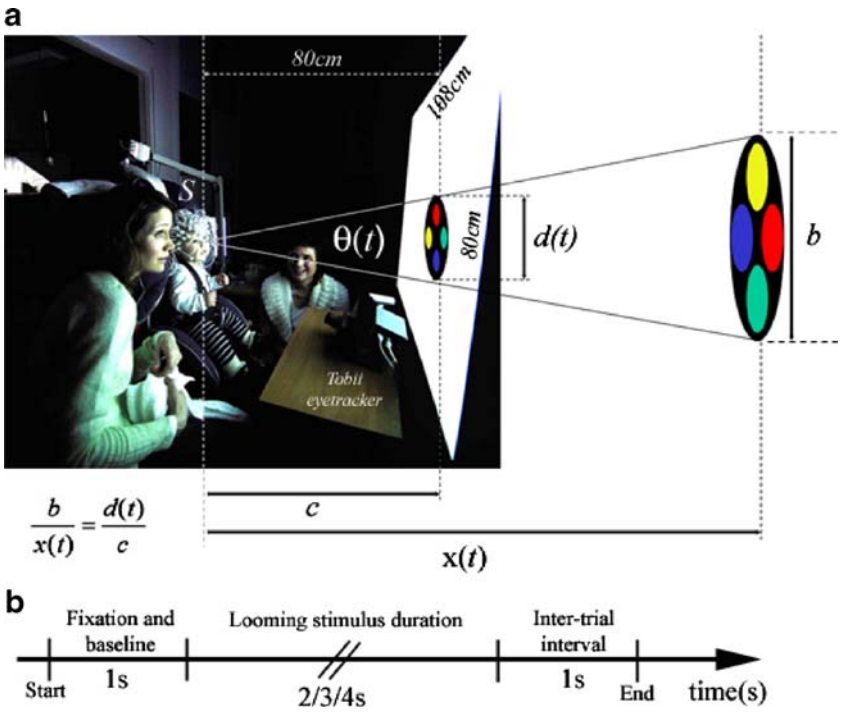

Fig. 1 The experimental setup and diagram of stimulus configuration (**a**) and procedure (**b**). Each infant was shown a semi-randomised sequence of an image of a circular disc on a collision course. As the virtual object approaches the eye, its image size on the screen grows. The looming stimulus simulated an object coming from far away (subtending 5° at the eye, θ) approaching for a duration of 2, 3 and 4 s under three different constant accelerations (21.1, 9.4 and 5.3 m/s^2, respectively) and finally 'hitting' the infants in the face (θ=131°). Movement stopped when the image filled the entire screen

of multiple equivalent dipolar sources by calculating the scalp distribution that would be obtained for a given dipole model (forward solution) and comparing it to the original visual evoked potential (VEP) distribution. Interactive changes in the location and orientation in the dipole sources lead to minimisation of the residual variance between the model and the observed spatiotemporal VEP distribution (Scherg 1990).

Here, we used a symmetrical VEP surrogate source model (Scherg 2002) consisting of 10 regional sources and seven dipoles, which we later for simplicity reduced to a three-dipole model of the visual areas consisting of standard 10–20 sites O1, Oz and O2. Dipoles at these sites were fitted around peak looming VEP activity, providing source waveforms (SWF) of the modelled brain regions as a direct measure of their activities on a trial-by-trial basis. Two particular dipoles, visual cortex lateral left (*VCrL*) and visual cortex lateral right (*VCrR*), showed consistent symmetrical synchronised activity in response to our looming stimulus. However, brain activity at dipole *VCrL* (see Supplementary Video 2) started earlier ($P<0.01$) and remained active longer ($P<0.01$).

To analyse the overall effect of looming on oscillatory neuronal synchronisation in dipole *VCrL*, a time–frequency analysis (Tallon-Baudry et al. 1998) on grand average data across age groups and loom speeds was performed, showing that evoked event-related oscillations in response to the looming stimulus predominantly took place within the theta range (Fig. 2). These findings are consistent with neurophysiological studies in humans showing that theta synchronisation in cortical structures plays an important role in attentional mechanisms providing the necessary conditions for an effective registration and processing of perceptual information (Vinogradova 1995; Pfurtscheller and Lopes da Silva 1999; Kahana et al. 2001).

By following the same procedure as in Hoechstetter et al. (2004), a four-shell ellipsoidal head model was created for every trial, and a predefined model of the visual cortex was inserted as dipoles into the head model. This model was then applied to the raw data transforming the EEG scalp signal to separate brain space signals (see Supplementary Fig. 1) resulting in a new EEG voltage sequence of the summed post-synaptic neuronal activity over time. The results of this analysis for the source waveform at dipole *VCrL* (Fig. 3a, dipole shown in head model in blue) are shown for the three infant age groups (Fig. 3b–d). Overall shape of the source waveforms was similar at the different ages. However, source waveform duration ranged from relatively short durations of about 50 ms in the 10–11-month-olds to twice as long durations in the 5–7-month-olds, revealing a significant developmental trend in processing time ($F(2, 15)=7.07$, $P<0.01$). A decrease in processing time with age has been reported before (Hollants-Gilhuijs et al. 2000; De Haan and Thomas 2002; Coch et al. 2005; Langrova et al. 2006) and is probably caused by a

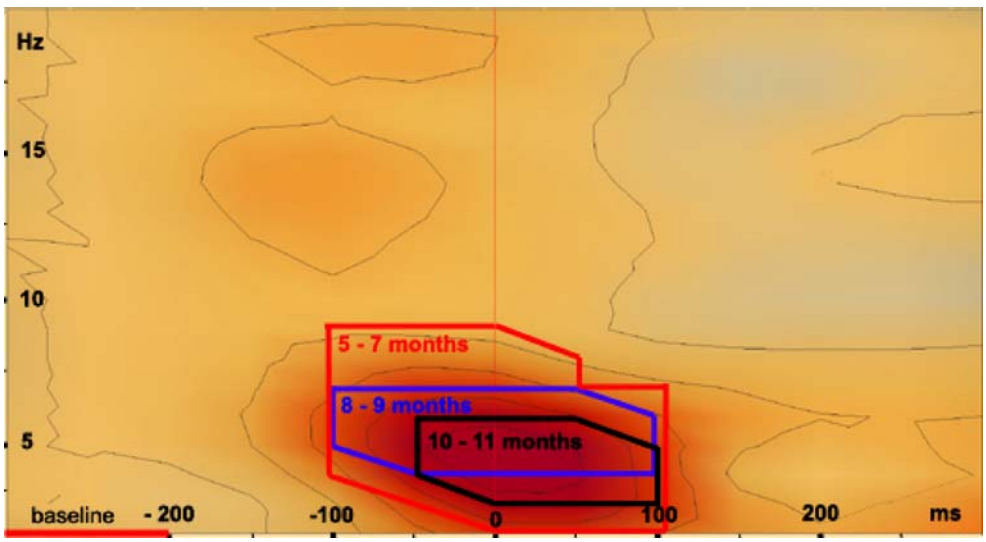

Fig. 2 Temporal–spectral evolution of percentage amplitude change at source *VCrL*. Time–frequency display of grand average data (across age groups and loom speeds) where the amplitude for each time instant is normalised to the mean amplitude of the baseline epoch for that frequency. To this end, individual looming trials were aligned by peak amplitude and analysed with an epoch length of −300:300 ms and a baseline of −300:−200 ms. Spectral change over time at dipole *VCrL* is indicated by the red cloud in the background indicating an overall 63% increase in activity between 0.1–7.5 Hz. The outlined areas in *red*, *blue* and *black* indicate where a significant increase in brain activity was found for the three age groups separately. These were between 0.1 and 8 Hz (delta/theta/alpha range) for the 5–7-month-olds ($P<0.001$), between 4 and 7 Hz (theta range) for the 8–9-month-olds ($P<0.001$) and between 2 and 6 Hz (delta/theta range) for the 10–11-month-olds ($P<0.005$)

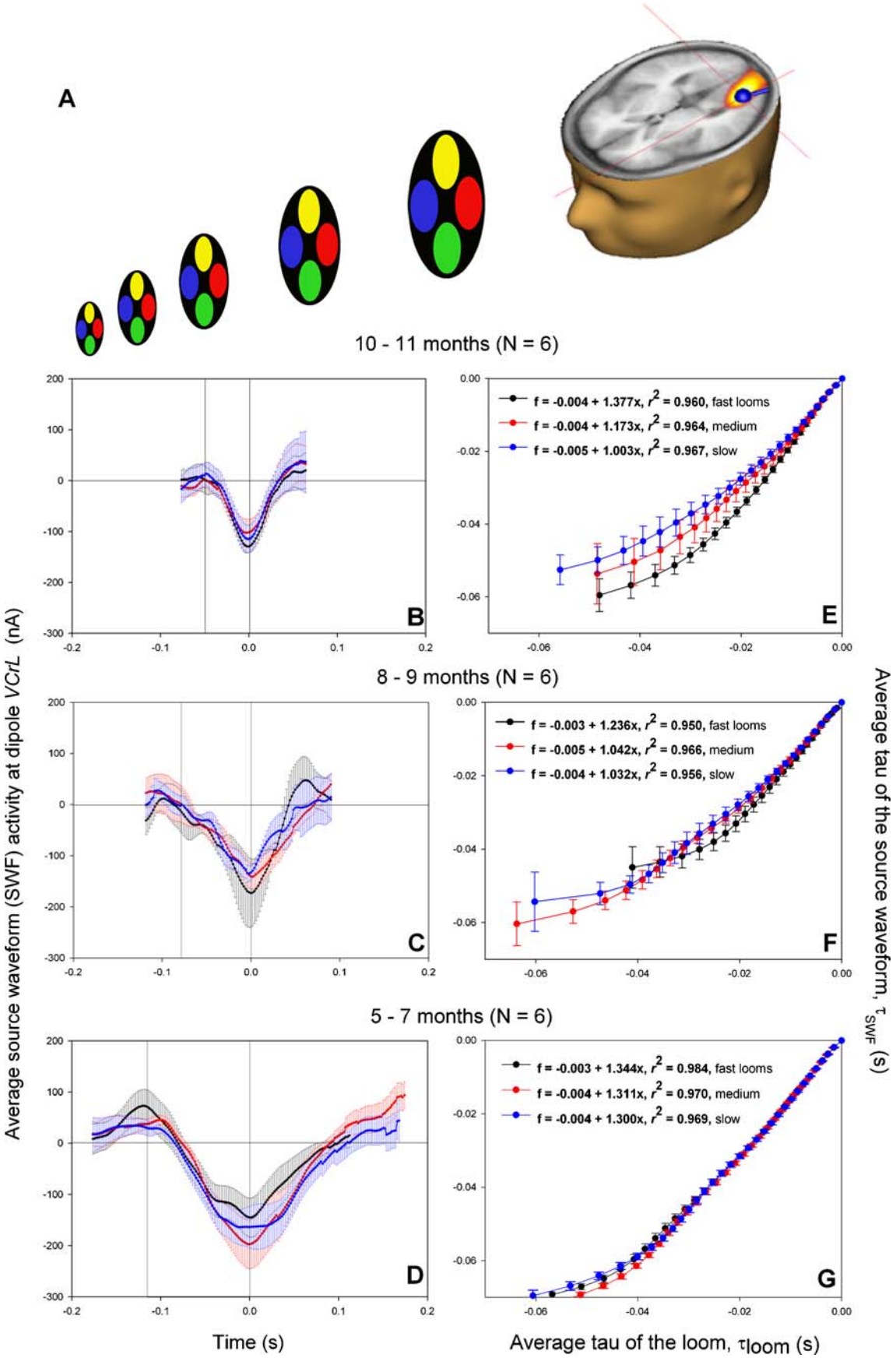
A
10 - 11 months (N = 6)
8 - 9 months (N = 6)
5 - 7 months (N = 6)
B
C
D
E
F
G
f = -0.004 + 1.377x, r2 = 0.960, fast looms
f = -0.004 + 1.173x, r2 = 0.964, medium
f = -0.005 + 1.003x, r2 = 0.967, slow
f = -0.003 + 1.236x, r2 = 0.950, fast looms
f = -0.005 + 1.042x, r2 = 0.966, medium
f = -0.004 + 1.032x, r2 = 0.956, slow
f = -0.003 + 1.344x, r2 = 0.984, fast looms
f = -0.004 + 1.311x, r2 = 0.970, medium
f = -0.004 + 1.300x, r2 = 0.969, slow
Average source waveform (SWF) activity at dipole VCrL (nA)
Time (s)
Average tau of the loom, τloom (s)
Average tau of the source waveform, τSWF (s)

Fig. 3 **a** Accelerating looming stimulus approaching the infants' eyes resulting in increased theta activity in the visual cortex. A four-shell ellipsoidal head model was created for every trial and used as a source montage to transform the recorded EEG data from electrode level into brain source space. The results of this analysis for dipole *VCrL* (depicted in head model in *blue*) are shown for the three infant age groups (**b**–**d**). Each *graph* shows averaged, peak-aligned source waveform activity at dipole *VCrL* (including standard error bars) for the three looms. Overall shape of the source waveforms was similar at the different ages, but their duration was about twice as long in the 5–7-month-olds as compared to the 10–11-month-olds. Source waveform activity did not discriminate well between slow, medium and fast looms. Therefore, peak-to-peak source waveform activity was tau-coupled (Lee 1998; Lee et al. 2001) onto the corresponding part of the loom to study the temporal dynamics of post-synaptic neuronal activity (see Fig. 4). **e**–**g** Average tau-coupling plots, τ_{SWF} vs τ_{loom} (including standard error bars), for each age group for the three loom speeds, showing that crawling 10–11-month-olds differentiated well between slow (in *blue*), medium (in *red*) and fast looms (in *black*), whereas younger pre-locomotor infants did not postnatal improvement of synaptic maturation and myelination (Grieve et al. 2003; Webb et al. 2005).

Source waveform activity per se did not discriminate well between slow, medium and fast looms. Therefore, we performed an extrinsic tau-coupling analysis (Lee 1998; Lee et al. 2001; Kayed and Van der Meer 2009) on the *VCrL* SWF. For each trial, SWF activity from the first positive to the first negative peak at dipole *VCrL* (i.e. the increase in summed post-synaptic neuronal activity in that particular brain region before it fades back to zero again) and its rate of change were plotted against time (Fig. 4a), as well as the corresponding visual angle of the looming stimulus and its rate of change (Fig. 4b). The peak velocity of each SWF was identified and demarcated at 10%, or as close to 10% as possible, of this value. The tau of the peak-to-peak SWF activity (τ_{SWF}) and the corresponding tau of

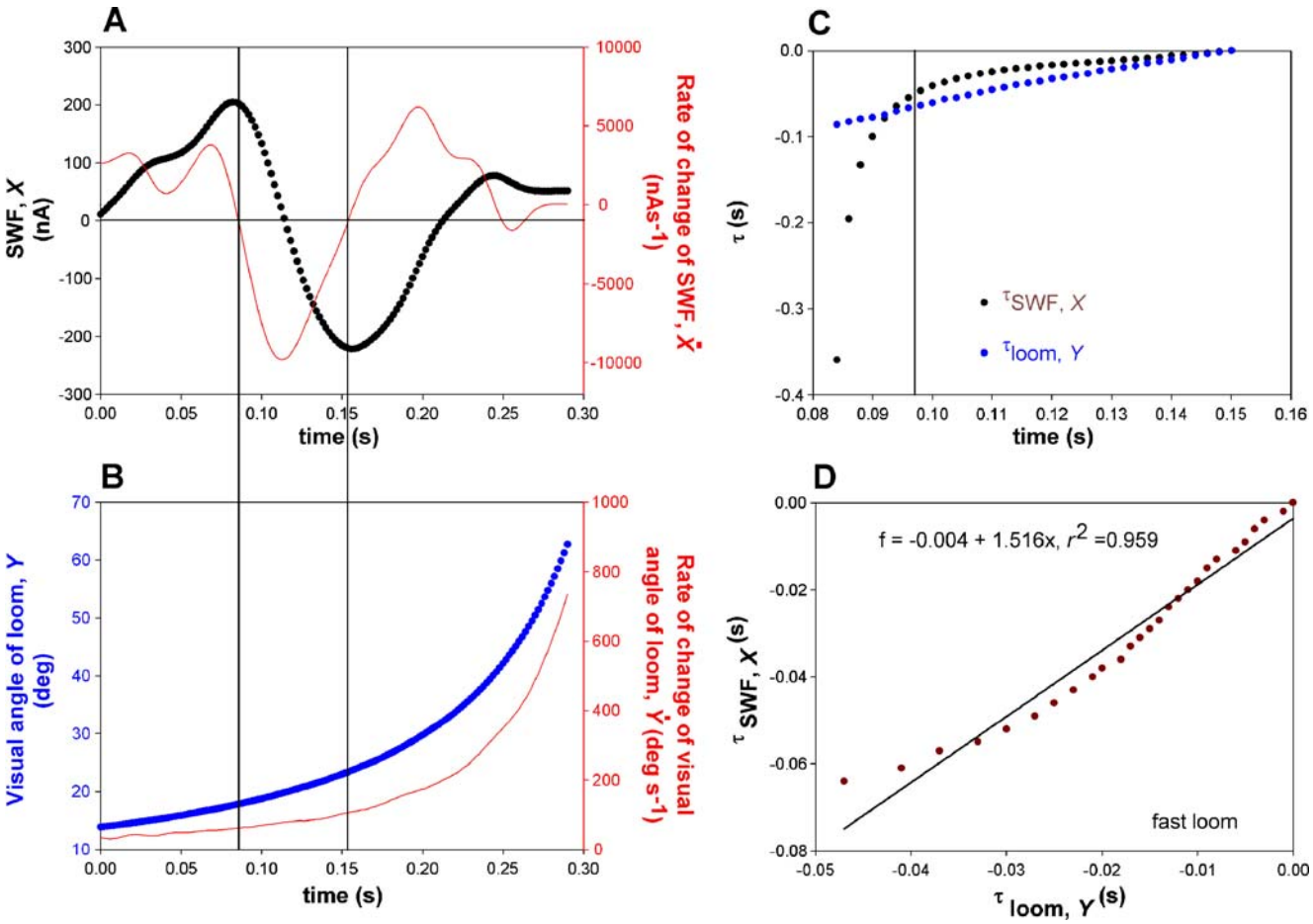

Fig. 4 Tau-coupling analysis. Two variables, X and Y, are tau-coupled if $\tau_{(X)}=K\tau_{(Y)}$, where K is a coupling constant. **a** Showing how SWF activity, X, and its rate of change, $\dot{X}$, changed continuously during a typical 11-month-old infant's brain response to a fast loom (21.1 m/s^2). **b** Showing how the visual angle of the looming stimulus, Y, and its rate of change, $\dot{Y}$, increased continuously during the loom's progression. The tau of peak-to-peak SWF activity ($\tau_{(X)}$, or $X/\dot{X}$, area between *vertical lines*) is plotted against time in **c** together with the corresponding tau for the loom ($\tau_{(Y)}$, or $Y/\dot{Y}$). **d** Plotting $\tau_{(X)}$ against $\tau_{(Y)}$ in order to find the percentage tau-coupling by means of a recursive linear regression. To ensure that 95% of the variance in the data was explained by a linear model, only regression strengths of $r^2>0.95$ were accepted, meaning that the first seven data points from the original data set were omitted. The remaining points in the plot were divided by the total number of points, providing an estimate of how much of the SWF's peak-to-peak activity was tau-coupled to the corresponding part of the loom. Here, percentage tau-coupling was 79.4%, r^2 of the coupling 0.959 and the regression slope 1.516

the loom (τ_{loom}) were calculated using the general equation: $\tau(x) = x/\dot{x}$ (Fig. 4c) and plotted against each other (Fig. 4d). Finally, a recursive linear regression analysis was run on the plot to determine the strength of the coupling between τ_{SWF} and τ_{loom} (measured by the r^2 value of the regression) and to estimate the value of the constant K in the tau-coupling equation $\tau_{SWF}=K\tau_{loom}$ (measured by the slope of the regression), by removing the leftmost points in the plot one by one until the r^2 of the regression exceeded the criterion level which was set at 0.95, thus ensuring that 95% of the variance in the data was explained by a linear model. The percentage of the SWF's peak-to-peak activity during which it is tau-coupled to the corresponding part of the loom was calculated by dividing the remaining points in the plot by the total number. For the data presented in Fig. 4d, the percentage tau coupling was 79.4%, the r^2 of the tau coupling was 0.959 and the regression slope was 1.516. High percentages of extrinsic tau-coupling and high r^2 values allow for the regression slope to be a good estimator of the coupling constant K.

Averaged time-normalised tau-couplings are shown for the three looms for each of the three infant age groups separately (Fig. 3e–g). In general, percentages tau-coupling were high, on average 69.9% (SD=9), 65.4% (SD=11) and 66.4% (SD=10) for the 10–11, 8–9 and 5–6-month-old infants, respectively. There was a small but not significant increase in percentage tau coupling with lower loom speeds from 64.7% (SD=9) to 67.7% (SD=11) to 69.3% (SD=9). Values of K were significantly >1 for all age groups and all loom speeds (slow: $t(17)=3.03$, $P<0.01$; medium: $t(17)=3.95$, $P<0.005$; fast: $t(17)=6.64$, $P<0.001$), reflecting well the accelerating nature of our looming stimulus which hit the infants in the face at high velocity. When $K>1$, as in our case, the buildup of peak-to-peak SWF activity at dipole *VCrL* ends with progressively increasing acceleration. In comparison, K values between $0<K<1$ would indicate that maximum negative SWF activity was reached whilst decelerating (see Lee 1998 for mathematical proof). A repeated measures ANOVA revealed a significant loom × group interaction ($F(4, 30)=3.225$, $P<0.03$), indicating that the 10–11-month-olds differentiated well between the three loom speeds with increasing values of K for faster looms, whilst the younger infants did not. Especially the 5–7-month-old infants, judging by their K values all lying around 1.3, appeared to process all looms as if they were fast looms (Fig. 3g). These findings suggest well-established neural networks for registering impending collision in 10–11-month-old, but not yet in 5–7-month-old infants. The 8–9-month-old infants displayed an in-between developmental stage. This could be interpreted as a sign that appropriate neural networks are in the process of being established and that the age of 8–9 months would be an important age for doing so. Coincidentally, this is also the average age at which infants start crawling. This makes sense from a perspective where brain and behavioural development go hand in hand (Johnson 2000). Namely, as infants gain better control of self-produced locomotion, their perceptual abilities for sensing looming danger improve.

We propose that as a function of perceptuomotor development, the temporal structure of looming information is increasingly well differentiated in the neural circuitry of the infant brain, providing infants with important time-to-collision information. Source waveform activity per se did not differentiate between loom speeds. However, when relating source waveform activity to its rate of change, using tau, and coupling this to the tau of the corresponding part of the loom, there was evidence of strong ($r^2>0.95$) and long (>65%) tau-coupling in all infants, where the 10–11-month-old infants in their brain activity clearly displayed a temporal structure that was consistent with that present in the visual looming information. Our results suggest that in the course of development, when looming-related post-synaptic current is flowing inside the neurons in a particular brain region, infants' ability to pick up the current flow's temporal structure improves, providing them with increasingly veridical time-to-collision information. Judging from the spatial location and temporal progression of our *VCrL* dipole, a likely area for processing this type of information would be where brain signals are progressing from visual cortical area V1 to V3 and V5/MT+, the (extra)striate areas (cf. Di Russo et al. 2005).

Acknowledgements We are grateful to all the infants and their parents for taking part in this study. We also thank D. N. Lee for discussion, G. -J. Pepping for providing us with the tau analysis software, S. Houweling and J. F. Léger for programming the looming stimuli and M. Holth for testing assistance.

References

Assmus A, Marshall JC, Ritzl A, Noth J, Zilles K, Fink GR (2003) Left inferior parietal cortex integrates time and space during collision judgments. NeuroImage 20:S82–S88

Coch D, Skendzel W, Grossi G, Neville H (2005) Motion processing in school-age children and adults, an ERP study. Dev Sci 8:372–386

Coull JT, Vidal F, Goulon C, Nazarian B, Craig C (2008) Using time-to-contact information to assess potential collision modulates both visual and temporal prediction networks. Frontiers in Human Neurosci 2:1–12

De Haan M, Thomas M (2002) Application of ERP and fMRI techniques to developmental science. Dev Sci 5:335–343

Di Russo F, Pitzalis S, Spitoni G, Aprile T, Patria F, Spinelli D, Hillyard SA (2005) Identification of the neural sources of the pattern-reversal VEP. NeuroImage 24:874–886

Dougherty RF, Koch VM, Brewer AA, Fischer B, Modersitzki J, Wandell BA (2003) Visual field representations and locations of visual areas V1/2/3 in human visual cortex. J Vision 3:586–598

Field DT, Wann JP (2005) Perceiving time to collision activates the sensorimotor cortex. Curr Biol 15:453–458

Gilmore RO, Baker TJ, Grobman KH (2004) Stability in young infants' discrimination of optic flow. Dev Psychol 40:259–270

Grieve PG, Emerson RG, Fifer WP, Isler JR, Stark RI (2003) Spatial correlation of the infant and adult electroencephalogram. Clin Neurophysiol 114:1594–1608

Hatsopoulos N, Gabbiani F, Laurent G (1995) Elementary computation of object approach by a wide-field visual neuron. Science 270:1000–1003

Hoechstetter K, Bornfleth H, Weckesser D, Ille N, Berg P, Scherg M (2004) BESA source coherence: a new method to study cortical oscillatory coupling. Brain Topogr 16:233–238

Hollants-Gilhuijs MAM, De Munck JC, Kubova Z, Van Royen E, Spekreijse H (2000) The development of hemispheric asymmetry in human motion VEPs. Vis Res 40:1–11

Holliday IE, Meese TS (2005) Neuromagnetic evoked responses to complex motions are greatest for expansion. Int J Psychophysiol 55:145–157

Johnson MH (2000) Functional brain development in infants: elements of an interactive specialization framework. Child Dev 71:75–81

Kahana MJ, Seelig D, Madsen JM (2001) Theta returns. Curr Opin Neurobiol 11:739–744

Kayed NS, Van der Meer ALH (2007) Infants' timing strategies to optical collisions: a longitudinal study. Infant Behav Dev 30:50–59

Kayed NS, Van der Meer ALH (2009) A longitudinal study of prospective control in catching by full-term and preterm infants. Exp Brain Res 194:245–258

Langrova J, Kuba M, Kremlacek J, Vit F (2006) Motion onset VEPs reflect long maturation and early ageing of visual motion-processing system. Vis Res 46:536–544

Lee DN (1998) Guiding movement by coupling taus. Ecol Psychol 10:221–250

Lee DN, Georgopoulos AP, Clark MJO, Craig CM, Port NL (2001) Guiding contact by coupling the taus of gaps. Exp Brain Res 139:151–159

Maier JX, Ghazanfar AA (2007) Looming biases in monkey auditory cortex. J Neurosci 27:4093–4100

Martinoya CJ, Delius D (1990) Perception of rotating spiral patterns by pigeons. Biol Cybern 63:127–134

Mehta MR, Lee AK, Wilson MA (2002) Role of experience and oscillations in transforming a rate code into a temporal code. Nature 417:741–746

Morrone MC, Tosetti M, Montanara D, Fiorentini A, Cioni G, Burr DC (2000) A cortical area that responds specifically to optic flow, revealed by fMRI. Nature Neurosci 3:1322–1328

O'Keefe J, Recce ML (1993) Phase relationship between hippocampal place units and the EEG theta rhythm. Hippocampus 3:317–330

Orekhova EV, Stroganova TA, Posikera IN (1999) Theta synchronization during sustained anticipatory attention in infants over the second half of the first year of life. Int J Psychophysiol 32:151–172

Pfurtscheller G, Lopes da Silva FH (1999) Event-related EEG/MEG synchronization and desynchronization: basic principles. Clin Neurophysiol 110:1842–1857

Ptito M, Kupers R, Faubert J, Gjedde A (2001) Cortical representation of inward and outward radial motion in man. NeuroImage 14:1409–1415

Rind FC, Simmons PJ (1997) Signaling of object approach by the DCMD neuron of the locust. J Neurophysiol 77:1029–1033

Scherg M (1990) Fundamentals of dipole source potential analysis. In: Grandori F, Hoke M, Romani GL (eds) Auditory evoked magnetic fields and electric potentials: advances in audiology. Karger, Basel, pp 40–69

Scherg M (2002) Advanced tools for digital EEG review: virtual source montages, whole-head mapping, correlation, and phase analysis. J Clin Neurophysiol 19:91–112

Schiff W (1965) Perception of impending collision: a study of visually directed avoidant behavior. Psychol Monogr 79:1–26

Schiff W, Caviness JA, Gibson JJ (1962) Persistent fear response in rhesus monkeys to the optical stimulus of "looming". Science 136:982–983

Shirai N, Yamaguchi MK (2004) Asymmetry in the perception of motion-in-depth. Vis Res 44:1003–1011

Sun H, Frost BJ (1998) Computation of different optical variables of looming objects in pigeon nucleus rotundus neurons. Nature Neurosci 1:296–303

Tallon-Baudry C, Bertrand O, Perronnet F, Pernier J (1998) Induced gamma-band activity during the delay of a visual short-term memory task in humans. J Neuroscience 18:4244–4254

Tucker DM (1993) Spatial sampling of head electric fields: the Geodesic sensor net. Electroencephalogr Clin Neurophysiol 87:154–163

Vinogradova OS (1995) Expression, control, and probable functional significance of the neuronal theta-rhythm. Prog Neurobiol 45:523–583

Webb SJ, Long JD, Nelson CA (2005) A longitudinal investigation of visual event-related potentials in the first year of life. Dev Sci 8:605–616